



## The effects of sunflower seed shell modifying process on textile dye adsorption: kinetic, thermodynamic and equilibrium study

Beyhan Kocadagistan\*, Erdem Kocadagistan

*Engineering Faculty, Environmental Engineering Department, Ataturk University, 25240 Erzurum, Turkey, Tel. +90 442 2314808; email: beyhank@atauni.edu.tr (B. Kocadagistan), Tel. +90 442 2314813; email: myecem@atauni.edu.tr (E. Kocadagistan)*

Received 9 April 2014; Accepted 18 October 2014

### ABSTRACT

This study investigates the effects of natural sunflower seed shells (NSS) modifying process on the adsorption of a basic dye. For this purpose, adsorption studies were carried out with acid ( $H_2SO_4$ ) treated shells and results were compared with that of NSS obtained in our previous studies. Common isotherm models were tested to evaluate the adsorption behaviours. It is concluded that Langmuir isotherm model is more suitable for modified NSS (MSS). The constants of this model were obtained as  $q_{max} = 284.45$  mg/g and  $b = 0.017$  L/mg for MSS at 30°C. The thermodynamic parameters were calculated as  $\Delta H^\circ = 76.24$  kJ/mol,  $\Delta S^\circ = 336.21$  J/mol and maximum  $\Delta G^\circ = -25.45$  kJ/mol. The adsorption process was followed by the pseudo-second-order equation according to the kinetic studies. Optimum pH and adsorbent dosage were calculated as 7.4 and 10 g/L, respectively, for adsorption of astrazon red (AR) on MSS in this study. Final dye concentrations in low-cost MSS decreased at least 45% that of NSS. The dye removal efficiencies were about 99% and the best weight per volume ratio (W/V) of MSS was 4.71 g MSS/L. More suitable and improved data were observed almost in all studied parameters with the adsorbent of MSS.

*Keywords:* Modified adsorbent; Adsorption; Astrazon red; Acid treatment

### 1. Introduction

Water pollution due to textile industrial effluents is one of the major concerns because of their toxicity and threat for human life. Over 10,000 dyes with an annual production over  $7 \times 10^5$  metric tons are commercially available world-wide and 5–10% of the dye stuff is lost in the industrial effluents [1].

The sorption process, for the treatment of polluted aqueous effluents, allows flexibility in design and operation, and produces aesthetically superior effluent suitable for re-use, free of pollutant in comparison

with the other used processes [2]. The major advantages of an adsorption system for water pollution control is more preferable in terms of both initial cost and land, simple design and easy operation, and it shows no effect of toxic substances compared to conventional biological treatment processes [3]. Because the high cost of commercial activated carbon, low-cost adsorbents have been investigated by researchers such as tea waste [4], silver wood sawdust carbon [5], rice husk carbon [6], orange peels [7], sea shell [8] and coconut coir dust [9].

Furthermore, researchers have investigated the modified adsorbents such as surface modified silicate mineral [10], hydrothermally modified fly ash [11],

\*Corresponding author.

Chitosan-modified palygorskite [12], modified zeolite [13], modified clay [14] and modified sugar cane bagasse [15] instead of its natural form to keep the operation costs at lower levels.

The purpose of this study is to investigate the effects of modifying process by acid treatment, applied to natural sunflower seed shells, removal of textile dye from wastewaters with adsorption technic.

## 2. Materials and methods

### 2.1. Adsorbate

Astrazon red GTLN (AR), which is supplied by Dystar Thai Co. Ltd, was used in this study to make an exact comparison with NSS used in our previous work. AR consists of two main components, which are C.I. basic yellow 28 and C.I. basic red, 18:1. The ratio of the two components is approximately 1:40 by weight. The molecular formula of AR is  $C_{19}H_{25}ClN_5O_2$ . The chromophoric system of AR dye consists of an azo group,  $-N=N-$  is in association with one or more aromatic systems [16] (Fig. 1).

### 2.2. Adsorbent

The NSS, used in this study, grinded to 1–2 mm sieve mesh size after they are washed with distilled water and dried at  $105^\circ\text{C}$  for 4 h at drying oven. Grinded SSS particles were treated with concentrated sulphuric acid 1:2 (w/v) for 36 h to achieve more activated surface with micropores. Then, the mixture was heated and then dried in a combustion furnace at  $105^\circ\text{C}$ . At the end of the acid treatment process, SSS particles (now considered as MSS) were washed with distilled water for several times. SEM photograph of MSS is given in Fig. 2.

Zeta potential and BET surface area values of SSS were determined by The Marmara Research Centre Material Institute of Scientific and Technological Research Council of Turkey (TUBITAK-MAM) using a Malvern Nanosize ZS-3600 model zeta meter and Nova 4000E model multipoint analyser, respectively. The multi-point BET surface area of NSS had been found as  $10.4\text{ m}^2$  in our previous study [17] while that of MSS was found as  $24.2\text{ m}^2$  in the current study.

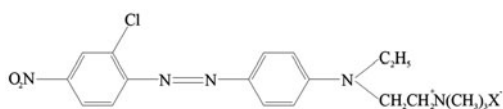


Fig. 1. Chemical structure of astrazon red GTLN  $124 \times 28\text{ mm}$  ( $300 \times 300\text{ DPI}$ ).

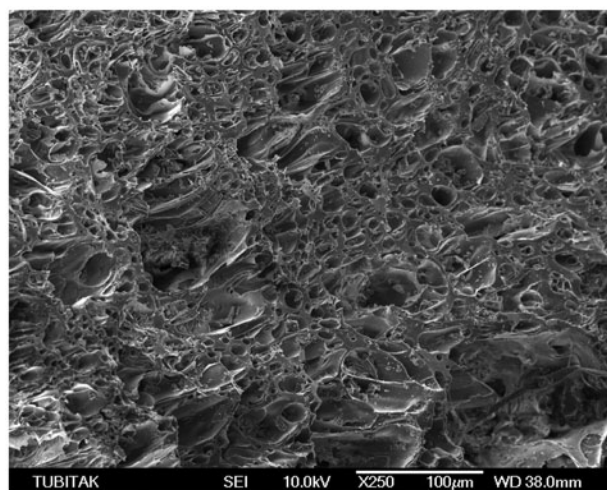


Fig. 2. SEM picture of NSS (upsizing =  $250\times$ )  $337 \times 270\text{ mm}$  ( $96 \times 96\text{ DPI}$ ).

Pore volume values of NSS and MSS are  $0.003843$  and  $0.005862\text{ cm}^3/\text{g}$ , respectively. Also, the isoelectric titration values (zetapotentials) of SSS are given in Table 1.

### 2.3. Experimental procedure

$0.15$  to  $1\text{ g}$  amounts of MSS and  $25$  to  $100\text{ mg/L}$  concentrations of AR dye solutions were added to the  $250\text{ mL}$  stoppered glass Erlenmeyer flasks during this study. The pH of the contents were measured with WTW Multi 340i model multiparameter device and kept between  $7$  and  $12$  for each experiment by adding

Table 1

Zeta potential and dye removal efficiencies according to different pH values

pH	Zeta potentials (mV)	Adsorption efficiencies (%)	
		NSS	MSS
1.25	-0.80	12.15	13.12
1.8	-1.75	14.21	16.13
2	-1.90	21.60	23.24
3	-5.50	37.50	42.05
3.85	-6.54	56.54	53.15
4.75	-8.30	59.86	66.07
6.25	-8.20	69.04	82.38
7.4	-10.90	95.01	98.92
9.25	-10.80	80.02	86.15
10.8	-14.00	78.00	81.28
12	-14.10	76.35	80.43

Note: Dye conc. =  $100\text{ mg/L}$ , adsorbent conc. =  $10\text{ g/L}$ , Agitat. time =  $120\text{ min}$ , Agitat. speed =  $200\text{ rpm}$ , Temp. =  $30^\circ\text{C}$ .

0.1 N NaOH solutions. Experiments were performed in a heat adjustable shaker and carried out at the temperatures of 20, 25 and 30 ± 1 °C.

Shaking was provided with an agitation speed of 200 rpm. 1 to 200 min testing periods were applied. At the end of these periods, flask contents were filtered and then dye concentrations were measured by using a Shimadzu UV 160A model spectrophotometer with 487 nm wavelength.

FT-IR spectra were recorded on a Bruker Vertex 70 spectrophotometer by an attenuated total reflectance (ATR) module.

#### 2.4. Adsorption isotherms

The equilibrium amount of adsorbed substances ( $q_e$ ) was calculated as follows:

$$q_e = \frac{(C_0 - C_e) \cdot V}{m} \quad (1)$$

where  $C_0$  and  $C_e$  are the liquid-phase concentrations of dye (mg/L) at initial and equilibrium state, respectively,  $V$  is the volume of the solution (L) and  $m$  is the mass of dry sorbent (g).

- Langmuir isotherm

The isotherm constants of  $q_{max}$  (mg/g) and  $b$  (L/mg) can be defined as monolayer adsorption capacity and Langmuir constant, respectively [18]. These parameters can be determined from the intercept and slope of ( $m/x$ ) vs. ( $1/C_e$ ) plot according to the linear form of Langmuir model equation (Eq. (2)).

$$\frac{1}{q_e} = \left( \frac{1}{b \cdot q_{max}} \right) \left( \frac{1}{C_e} \right) + \left( \frac{1}{q_{max}} \right) \quad (2)$$

- Freundlich isotherm

$K_F$  and  $1/n$  isotherm constants of the entire system can be determined from the intercept and slope of  $\ln q_e$  vs.  $\ln C_e$  plot in compliance with Eq. (3) [18].

$$\ln(q_e) = \ln K_F + \frac{1}{n} \ln C_e \quad (3)$$

- Temkin isotherm

The linear form of Temkin isotherm is given in Eq. (4)  $A$  and  $B$  constants can be determined from the intersect and slope of  $q_e$  vs.  $\ln C_e$  plot.

$$q_e = \frac{RT}{b} \ln A + \frac{RT}{b} \ln C_e \quad (4)$$

where  $A$  (L/mg) represents the equilibrium binding and  $B$  (J/mol) is related to heat of sorption Temkin constants,  $R$  is the universal gas constant (8.314 J/mol K),  $T$  is the temperature in Kelvin and  $b$  is the Temkin isotherm constant [18].

### 3. Result and discussion

#### 3.1. Effect of pH

It was reported that adsorption efficiencies of basic dyes decreased at lower pH due to the occurrence of proton in acidic mediums [19]. Similarly, optimum pH value was found as 7.4 in our previous work [17]. In this study, various pH values between 1.25 and 12 were tested again to define the optimum pH value efficiently. The adsorption efficiencies of natural and modified shells at different pH values and zeta potentials are given in Table 1. As seen from this table, the zeta potential values were increased with increasing pH but more specifically from pH 6.25 to 7.4 and 9.25–10.8. Hence, subsequent experiments were concentrated around pH 7.4 and above.

As can be seen from Table 1, the adsorption efficiencies increase with the increasing pH up to 7.4, and it reaches to 95.01 and 98.92% for NSS and MSS, respectively. Lower efficiencies and zeta potential values were observed under this pH level, especially 3 and below. These lower values originate from the positive charges at the surface of the adsorbents when  $H^+$  ions become predominate at lower pH values. On the other hand, negatively charged surface of biomass enhances the positively charged dye cations through electrostatic attraction force [20] at higher pH levels. The weak solubility of AR dye at basic mediums is responsible for the low efficiency values at higher zeta-potentials after pH 7.4. zeta-potentials increase with increasing pH but adsorption efficiencies decrease with increasing pH above 7.4 (Table 1). As a result, optimum pH value was found as 7.4 in the adsorption of AR on to MSS.

The positive effect of shell modifying process is observed from Table 1. Dye adsorption efficiencies of MSS were higher at all pH than that of NSS.

#### 3.2. Comparison of adsorbent dosage and initial dye concentration effects

Adsorption efficiencies vs. adsorbent concentrations graphs are given in Fig. 3 for various initial dye amounts at optimum pH. They increase with

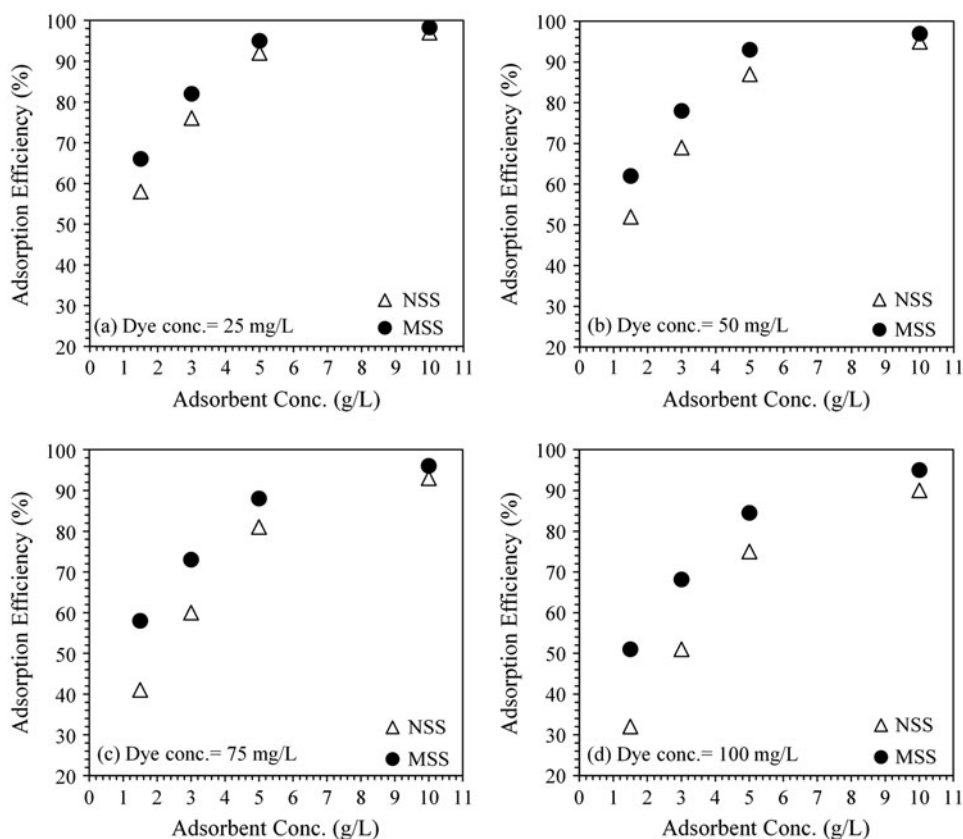


Fig. 3. Effect of NSS and MSS concentrations on the adsorption efficiencies for 25 (a), 50 (b), 75 (c) and 100 mg/L (d) initial dye concentrations (pH = 7.4, Agitat. time = 120 min, Agitat. speed = 200 rpm, Temp. = 30 °C).

increasing adsorbent concentrations at all applied initial dye concentrations. Although less adsorbent and higher dye concentrations applied to MSS, higher efficiencies are observed than that of NSS.

When 25 mg/L initial dye concentration was applied, dye removal efficiencies were observed as 66, 82, 95 and 98% at 1.5, 3, 5 and 10 g/L MSS concentrations, respectively. These efficiencies for same concentrations of NSS are 58, 76, 92 and 97%. The effects of modifying process on the adsorption performances of shells can be clearly seen from Fig. 3(a–d). When MSS is used as adsorbent, the dye removal efficiency is 58% with 1.5 g/L MSS and 75 mg/L initial AR dye (Fig. 3(c)). The same efficiency level with the same adsorbent dosage of NSS had been achieved with 25 mg/L AR concentration (Fig. 3(a)). Similarly, the adsorption efficiency of 95% was observed both with 10 g/L MSS and 100 mg/L initial AR dye (Fig. 3(d)) and 10 g/L NSS and 50 mg/L initial AR dye (Fig. 3(b)) studies. Also these results show that modifying process improves the AR dye adsorption capacity of sunflower seed shells.

Fig. 4 shows residual dye concentrations at the end of the processes. As can be seen from this figure, residual dye concentrations after adsorption, obtained with MSS, are lower than that of NSS. At the end of the experiments (120 min), unadsorbed dye concentrations are 0.44, 1.42, 2.71 and 4.52 mg/L for 25, 50, 75 and 100 mg/L initial AR concentrations, respectively, for the adsorbent of MSS. On the other hand, higher residual concentrations are obtained with NSS such as 0.75, 2.64, 5.51 and 10.21 mg/L, respectively, for the same initial dye concentrations. According to these results, residual AR dye concentrations, observed with the adsorbent of MSS, were less as much as 43–56% of NSS. This means that the amount of discharged AR dye to the water bodies could be reduced to 49% on average.

### 3.3. Comparison of isotherm parameters

The plots of adsorption models at  $T = 30^{\circ}\text{C}$  are given in Fig. 5. Langmuir (Fig. 5(a)) Freundlich (Fig. 5(b)) and Temkin (Fig. 5(c)) isotherms have been

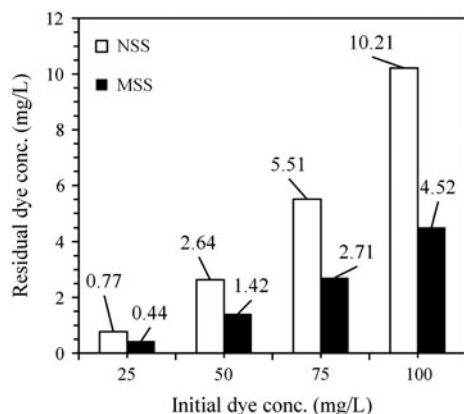


Fig. 4. Residual dye concentrations for various initial concentrations of AR dye (pH = 7.4, adsorbent conc. = 10 g/L, Agitat. speed = 200 rpm, Temp. = 30°C) 64 × 53 mm (300 × 300 DPI).

used to describe the equilibrium adsorption characteristics of NSS and MSS.

The Freundlich and Langmuir isotherm models assume a heterogeneous surface and specific homogeneous sites within surfaces, respectively, where the sorption takes place. Different from those models, the Temkin isotherm assumes that the heat of adsorption of all the molecules in a layer decreases linearly due to adsorbent–adsorbate interactions. This adsorption is characterized by a uniform distribution of binding energies up to some maximum binding energy [21]. The entire isotherm parameters calculated in this study are shown in Table 2, to make a comparison between NSS and MSS. The correlation coefficients of these isotherm models were also determined.

The constant of Freundlich ( $n$ ) is an indicator for the satisfactoriness of adsorption. When it is in the range of 1–10, adsorption processes is accepted as

favourable [22]. It was in the range of 1.089–1.189 for NSS and 1.367–1.426 for MSS in this study (Table 2). As a result, MSS can be accepted as more useful adsorbent than NSS to remove AR dye from wastewaters based on these values.

Dimensionless separation factor of  $R_L$  was determined using with highest initial concentration of  $C_o$  and isotherm constant of  $b$  (Eq. (5)), to indicate the feasibility of adsorption process from the point of Langmuir theory. According to this theory, adsorption process can be considered as irreversible when  $R_L = 0$ , favourable when  $0 < R_L < 1$ , linear when  $R_L = 1$ , and unfavourable when  $R_L > 1$  [22].

This separation factor is given in Eq. (5).

$$R_L = \frac{1}{1 + bC_o} \quad (5)$$

$R_L$  values were found in the range of 0.208–0.360 with an average of 0.271 for NSS and 0.164–0.213 with an average of 0.240 for MSS (Table 2). The average values of  $R_L$  indicate that AR dye adsorption is favourable with both form of sunflower seed shells.

Determined Temkin isotherm constants ( $A$ ) of MSS were greater (6.64–7.94 L/g) than those of NSS (1.342–1.421 L/g) with the averages of 7.397 and 1.369 L/g, respectively. As can be seen from Table 2, Freundlich and Langmuir isotherms correlation coefficients of NSS adsorption studies are close to each other and almost 1 for all studied temperatures. Nevertheless,  $R^2$  value of 0.997 calculated by Langmuir at 30°C for NSS is higher than those of the Freundlich or Temkin equations. In the case of MSS, Langmuir produces more suitable data than the other isotherms since it has higher  $R^2$  values such as 0.973 or 0.970 at 20 and 30°C, respectively. According to these results, one can claim that the surface of MSS is almost homogeneous.

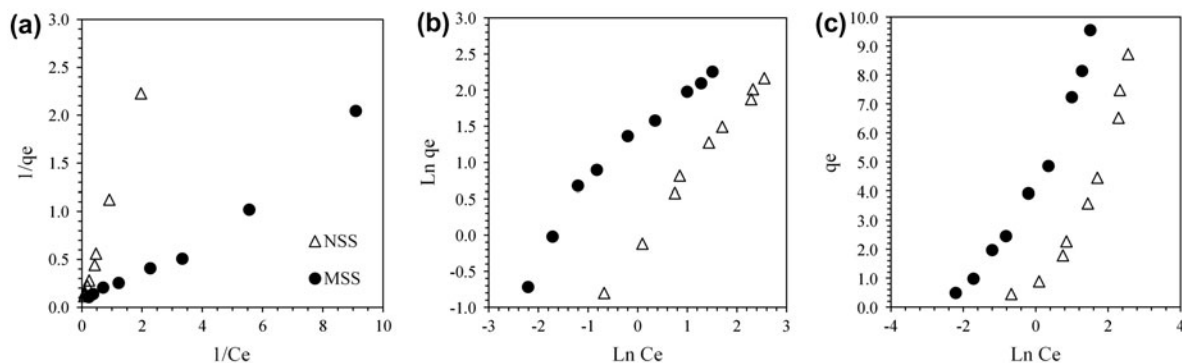


Fig. 5. Langmuir (a), Freundlich (b) and Temkin (c) isotherm models for the adsorption of AR onto SSS (pH 7.4,  $m = 10$  g/L, Agitat. speed = 200 rpm,  $T = 30^\circ\text{C}$ ) 70 × 22 mm (300 × 300 DPI).

Table 2  
Isotherm model constants for removal of AR at different temperatures

	NSS			MSS		
	20°C	25°C	30°C	20°C	25°C	30°C
<i>Langmuir</i>						
$q_{max}$ (mg/g)	22.80	29.26	47.45	79.29	101.13	<b>284.45</b>
$b$ (L/mg)	0.038	0.031	0.018	0.051	0.044	0.017
$R_L$	0.208	0.244	0.360	0.164	0.185	<b>0.370</b>
$R^2$	0.992	0.995	0.997	0.973	0.962	0.970
<i>Freundlich</i>						
$K_F$	0.934	1.001	0.925	3.344	3.512	<b>3.813</b>
$n$	1.189	1.186	1.089	1.369	1.427	<b>1.366</b>
$R^2$	0.994	0.992	0.993	0.960	0.948	0.956
<i>Temkin</i>						
$B$ (J/mol)	2.297	2.344	2.585	2.347	2.265	<b>2.379</b>
$b_T$	1,060	1,057	974	1,038	1,094	1,059
$A$ (L/g)	1.345	1.421	1.342	6.639	7.611	<b>7.940</b>
$R^2$	0.890	0.908	0.900	0.960	0.958	0.963

As shown in Table 2, maximum adsorption capacities increase with the increasing temperature and best results are obtained for all studied temperatures when MSS is used. For example, the  $q_{max}$  value of NSS (47.45 mg/g) one sixth of MSS (284.45 mg/g) at 30°C.

In addition, the entire isotherm parameters seem more favourable when MSS is used. This can be verified with the highest values of  $q_{max}$  and  $R_L$  of Langmuir,  $K_F$  and  $n$  of Freundlich and  $A$  and  $B$  of Temkin isotherms, all given as bold characters in Table 2.

These results confirm that modifying process of SSS makes MSS more suitable for the adsorption of AR dye.

### 3.4. Comparison of thermodynamic parameters

Many adsorption studies have been focused on the adsorption thermodynamics to identify the affinity of adsorbent for the adsorbate [23,24]. The thermodynamic parameters can be calculated using the following equations:

$$\Delta G^\circ = -RT \ln K \tag{6}$$

$$\Delta G^\circ = DH^\circ - TDS^\circ \tag{7}$$

where  $R$  is the universal gas constant (8.314 J/mol K),  $T$  is the temperature in Kelvin and  $K$  is the Langmuir constant (L/mol). Here,  $\Delta H^\circ$  and  $\Delta S^\circ$  values can be calculated from the intercept and slope of  $\Delta G^\circ$  vs.  $T$

plot (Eq. (7)). Table 3 shows the thermodynamic parameters for NSS and MSS.

The negative values of  $\Delta G^\circ$  indicate the spontaneity degree of the adsorption process [25]. These values indicate that the adsorption process of AR on NSS and MSS is favourable and spontaneous. On the other hand, the positive value of  $\Delta H^\circ$  and  $\Delta S^\circ$  shows that the process is endothermic in nature and increases randomly at the solid-solution interface. Entropy, in thermodynamics, is a measure of the number of specific ways in which a thermodynamic system may be arranged, commonly understood as a measure of disorder. The positive entropy change is due to the redistribution of energy between adsorbate and adsorbent [26], and it likely indicates the changes in the structure of adsorbents during adsorption [27]. It can be seen clearly from Table 3 that the modifying process of NSS has a positive effect on the adsorption of textile dye since the MSS have greater  $\Delta H^\circ$ ,  $\Delta S^\circ$  and lower  $\Delta G^\circ$  values.

### 3.5. Dynamics of adsorption

To examine the controlling mechanism or rate limiting step of the adsorption process, the pseudo-first- and second-order kinetic model rate expressions were applied to NSS and MSS. Pseudo-first-order equation is also known as the Lagergen equation and based on solid capacity [28]. On the other hand, the pseudo-second-order kinetic model is based on adsorption equilibrium capacity [29]. Linear form of these models [30] are given in Eqs. (8) and (9).

$$\log(q_e - q_t) = \log q_e - \frac{k_1}{2.303}t \tag{8}$$

$$\frac{t}{q_t} = \frac{1}{k_2 q_e^2} + \frac{1}{q_e}t \tag{9}$$

where  $k_1$  (1/min) and  $k_2$  (g/mg min) are the adsorption rate constants of first-order and second-order

Table 3  
Thermodynamic parameters for the adsorption of AR onto NSS and MSS

T (°C)	$\Delta G^\circ$ (kJ/mol)		$\Delta H^\circ$ (kJ/mol)		$\Delta S^\circ$ (J/mol K)	
	NSS	MSS	NSS	MSS	NSS	MSS
20	-21.99	-22.09	26.41	76.24	165.42	336.21
25	-23.01	-24.13				
30	-23.65	-25.45				

kinetic models, respectively,  $q_e$  (mg/g) is the equilibrium adsorption uptake and  $q_t$  (mg/g) is the adsorption uptake at time  $t$ .

$k_1$ ,  $k_2$  and  $q_e$  parameters were calculated from the slope and intercept of  $\log(q_e - q_t)$  vs.  $t$  (Fig. 6) and  $t/q_t$  vs.  $t$  (Fig. 7) plots, respectively.

Table 4 represents the entire kinetic parameters of pseudo-first- and second-order models for the adsorption of AR dye onto NSS and MSS.

As can be seen from Table 4, pseudo-second-order model gives more favourable results than pseudo-first-order. The correlation coefficients of second-order model are close to 1 with all studied initial dye concentrations for NSS and MSS. These coefficients of first-order model are observed as small especially for low initial dye concentrations such as 25 and 50 mg/L. In addition, predicted values of  $q_{e_{cal}}$  were closer to the experimentally measured values of  $q_{e_{exp}}$  in pseudo-second-order models. According to these results, it is clear that pseudo-second-order model is a preferable model to describe the kinetics of AR dye adsorption for which

the rate is controlled by a chemi-sorption process of the both tested adsorbents of this study. The pseudo-second-order kinetic model is based on the sorption capacity on the solid phase, and it predicts the rate controlling step. As can be seen from Table 4, the better results are obtained with the pseudo-second-order model. The correlation coefficients ( $R^2$ ) of pseudo-second-order kinetic model are bigger than 0.99 for all initial dye concentrations and better than that of the first-order models.

The accuracy of model, applied to the mentioned adsorption, can be explained with an evaluation of differences between  $q_{e_{cal}}$  and  $q_{e_{exp}}$  values related to NSS and MSS. To clarify this idea  $q_{e_{exp}}/q_{e_{cal}}$  ratios are determined. Higher the  $q_{e_{exp}}/q_{e_{cal}}$  ratio, closer the  $q_{e_{cal}}$  and  $q_{e_{exp}}$  values. As can be seen from Fig. 8, mentioned ratios for NSS and MSS are in the range of 0.954–0.965 and 0.976–0.981, respectively. These values indicate a stronger relationship between experimental results and the model, especially for MSS. In other words, the predicted equilibrium sorption capacity

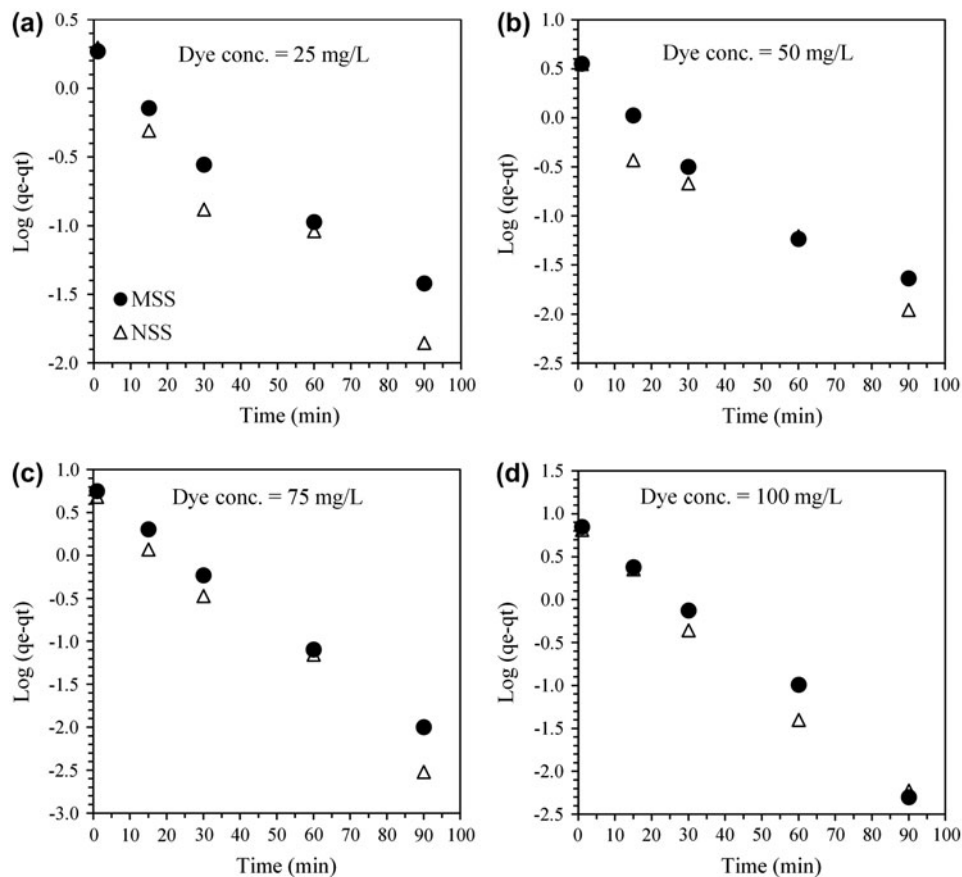


Fig. 6. Pseudo-first-order kinetic models for the adsorption of AR onto NSS for 25 (a), 50 (b), 75 (c) and 100 mg/L (d) initial dye concentrations (pH = 7.4,  $m = 10$  g/L, Agitat. speed = 200 rpm, T = 30 °C).

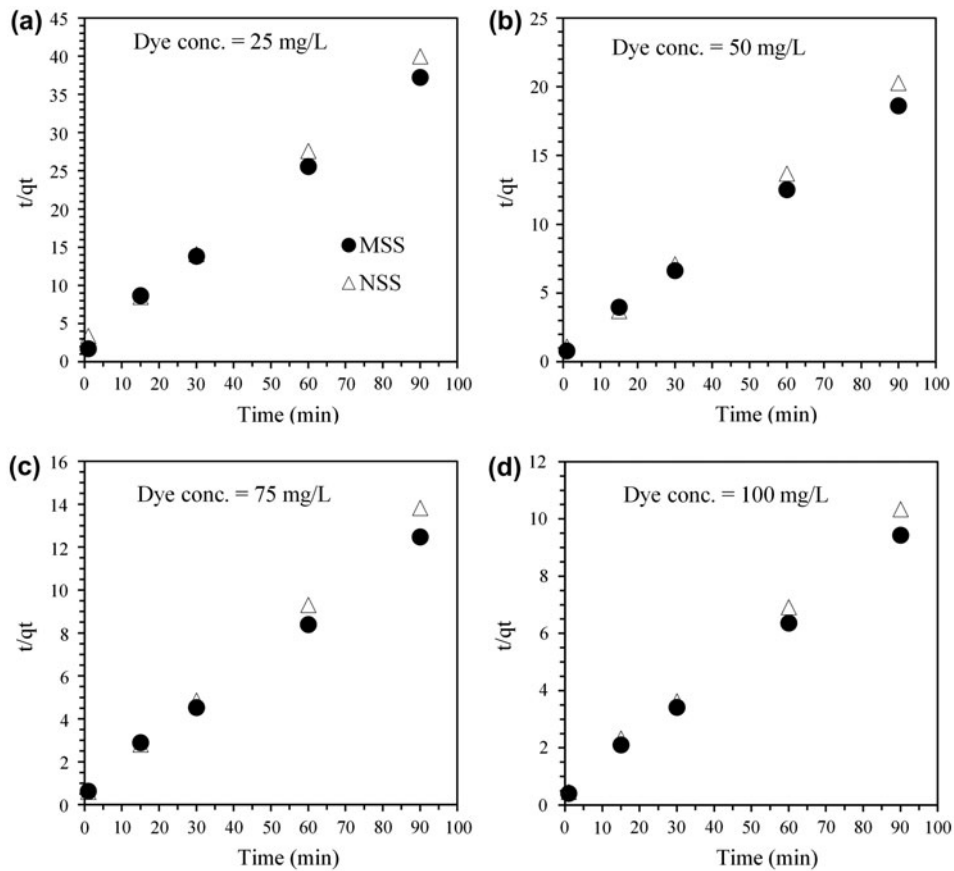


Fig. 7. Pseudo-second-order kinetic models for the adsorption of AR onto MSS for 25 (a), 50 (b), 75 (c) and 100 mg/L (d) initial dye concentrations (pH = 7.4,  $m = 10$  g/L, Agitat. speed = 200 rpm, T = 30°C).

Table 4  
The pseudo-first- and second-order kinetic parameters

$C_o$ (mg/L)	$qe_{exp}$ (mg/g)		$k_1$ (1/min)		$qe_{cal}$ (mg/g)		$R^2$	
	NSS	MSS	NSS	MSS	NSS	MSS	NSS	MSS
<i>Pseudo-first-order model</i>								
25	2.27	2.46	0.050	0.042	1.23	1.42	0.9274	0.9713
50	4.45	4.86	0.058	0.056	1.73	2.52	0.9337	0.9646
75	6.52	7.22	0.078	0.071	4.56	5.65	0.9855	0.9989
100	8.72	9.55	0.080	0.080	6.28	8.29	0.9927	0.9935
$C_o$ (mg/L)	$qe_{exp}$ (mg/g)		$k_2$ (1/min)		$qe_{cal}$ (mg/g)		$R^2$	
	NSS	MSS	NSS	MSS	NSS	MSS	NSS	MSS
<i>Pseudo-second-order model</i>								
25	2.27	2.46	0.082	0.093	2.38	2.52	0.9988	0.9986
50	4.45	4.86	0.081	0.076	4.56	4.96	0.9995	0.9995
75	6.52	7.22	0.049	0.041	6.70	7.36	0.9998	0.9987
100	8.72	9.55	0.029	0.040	9.04	9.77	0.9986	0.9990



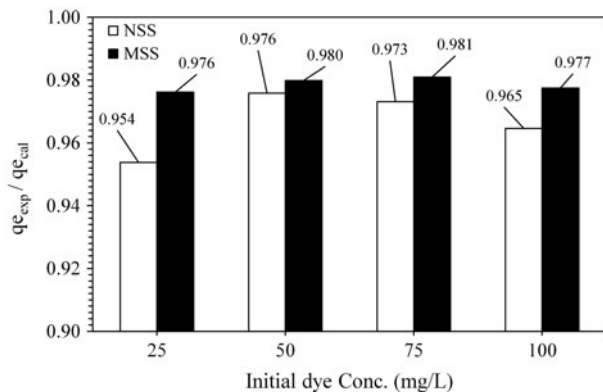


Fig. 8. The chart of  $q_{e,exp}/q_{e,cal}$  ratio vs. initial dye concentrations (pH = 7.4,  $m = 10$  g/L, Agitat. speed = 200 rpm,  $T = 30^\circ\text{C}$ )  $76 \times 45$  mm ( $300 \times 300$  DPI).

values show a good agreement with the experimental equilibrium uptake values.

### 3.6. Characterization of SSS

Fig. 9 represents the FT-IR spectrums of the astrazon red dye (a) and MSS after (b) and before (c) adsorption. The FT-IR spectra suggest that the adsorption mechanism could be considered as a combination of electrostatic interaction and physical sorption. The intense broad peaks at  $3462.18$   $\text{cm}^{-1}$  (b) and

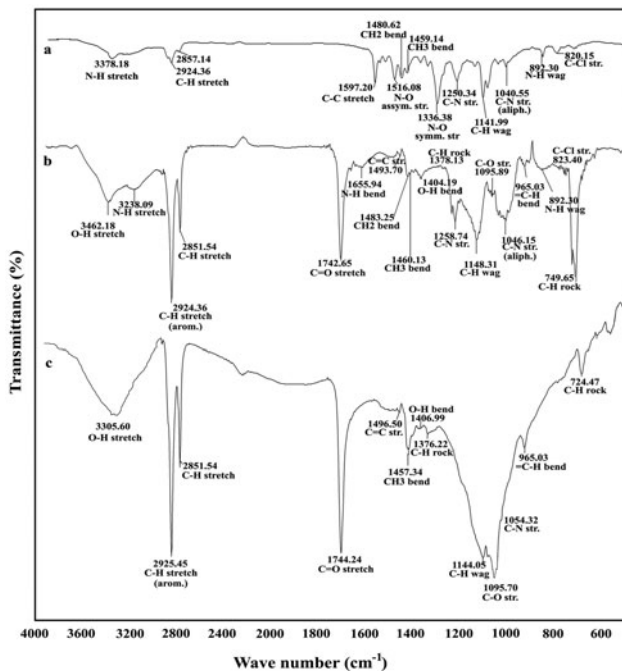


Fig. 9. FT-IR spectrums: Astrazon red dye (a), MSS after adsorption (b) and MSS before adsorption (c).

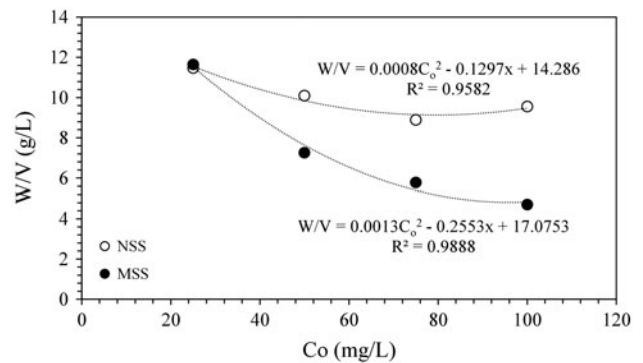


Fig. 10.  $W/V$  vs. initial AR concentrations (pH = 7.4, Agitat. speed = 200 rpm, Temp. =  $30^\circ\text{C}$ )  $76 \times 45$  mm ( $300 \times 300$  DPI).

$3305.60$   $\text{cm}^{-1}$  (c) are due to the O–H stretching vibration of the cellulose of SSS. The presence of aromatic components in the SSS is evidenced by a peak at  $2924.36$   $\text{cm}^{-1}$  (b) and  $2925.45$   $\text{cm}^{-1}$  (c) due to the C–H stretching vibration. The presence of oil is verified by its C=O vibration at  $1742.65$   $\text{cm}^{-1}$  (b) and  $1744.24$   $\text{cm}^{-1}$  (c).

Almost all of the peaks have different wavenumbers for the cases of (b) and (c) in Fig. 10. In addition, some peaks are disappeared or shifted while some new peaks are detected. This indicates the possible bindings of functional groups on the surface of the SSS during the adsorption process. The intensity and wavenumber of peaks were either reduced or slightly shifted after sorption of the dye. This can be attributed to the electrostatic interactions between the positively charged functional groups of the sorbent and the AR dye.

### 3.7. Cost assessment

Adsorbent cost is an important parameter for comparing the industrial application of adsorbent materials. However, it is rarely reported in the literature [31,32]. The overall cost of the adsorbent material is governed by several factors such as its availability (whether it is natural, industrial/agricultural/domestic wastes or by-products or synthesized products), requirement for processing required and its reusability [33]. Sunflower seed has an extensive usage in the oil industries such as cooking oil, margarine and biodiesel. Sunflower seed shell is a cost free product waste of these and similar industries.

Using with Eq. (1), the mass balance equation can be rearranged as below for the adsorption of dye process.

Table 5  
Experimental and calculated values of required MSS quantities for various initial dye concentrations at 30 °C

$C_o$ (mg/L)	$C_e$ (mg/L)	$W/V_{exp}$ (g/L)	$W/V_{cal}$ (g/L)
25	0.44	11.64	11.50
50	1.42	7.26	7.56
75	2.71	5.78	5.24
100	4.52	4.71	4.54

$$V(C_o - C_e) = W(q_e - q_o) = Wq_e \quad (10)$$

where  $q_o$  is the adsorption uptake (mg/g) at initial.

Since Langmuir gives the best fit to the experimental data on the adsorption of AR on MSS, Eq. (10) can be rearranged giving adsorbent/solution ratios for this system as follow:

$$\frac{W}{V} = \frac{C_o - C_e}{q_e} = \frac{C_o - C_e}{\left(\frac{q_m b C_e}{1 + b C_e}\right)} \quad (11)$$

The plot of  $W/V$  vs.  $C_o$  at 30 °C is given in Fig. 10. As can be seen from this plot, 9.56 g/LNSS is required for 100 mg/L initial dye concentration. This quantity decreases to 4.71 g MSS/L for same initial dye concentration. The strong relationship between  $W/V$  and  $C_o$  (Fig. 10) is observed with a polynomial equation (Eq. (12)).

$$\frac{W}{V} = 0.0013 C_o^2 - 0.1297 C_o + 17.0753 \quad (12)$$

Experimentally, observed and model based calculated values for MSS (Eq. (12)) are given in Table 5. According to this model, 4.54 kg MSS per one cubic meter of wastewater decreases the dye concentrations from 100 to 4.52 mg/L within 2 h.

Generally, the commercial activated charcoal, most commonly used and most effective adsorbent [34], costs about 1–2 \$ per kg in Europe. Compared to activated charcoal, the total cost of MSS is extremely low. After the adsorption process, the final MSS can be disposed via landfill or by incineration. Thus, it is thought that, the use of MSS as an adsorbent will be an economic attempt to remove the astrazon red textile dye from wastewaters.

#### 4. Conclusions

It was observed that modifying process of NSS improved the astrazon red GTLN adsorption

performance of NSS. Modified NSS (MSS) may be a good and low-cost adsorbent to remove AR dye from wastewaters.

Higher adsorption efficiencies are achieved with fewer adsorbate quantities and higher dye concentrations with MSS.

Experiments conducted with MSS resulted with higher adsorption efficiencies with less adsorbent and higher dye concentrations than those of NSS.

Isotherm studies showed that the Langmuir is more favourable than Freundlich and Temkin models as in the case with NSS. However, different values of isotherm parameters were observed with MSS. An extraordinary increase from 47.45 to 284.45 mg/g for NSS and MSS, respectively, in the maximum adsorption capacity ( $q_{max}$ ) of the Langmuir isotherm model at 30 °C. The other studied temperatures showed similar results. In addition,  $b$  constant of Langmuir model decreased from 0.018 to 0.017, and  $R_L$  separation factor of this model increased from 0.36 to 0.37 for NSS and MSS, respectively. In Freundlich isotherm model, the  $K_F$  constant increased from 0.934 to 3.344 at 20 °C and 0.925 to 3.813 at 30 °C when MSS used. Likewise, the  $n$  parameter is also increased. In Temkin model, the best values of  $A$  and  $B$  parameters were observed with MSS as 2.379 and 7.940 L/g, respectively, at 30 °C (Table 2).

The  $q_{cal}^e$  values, determined with the data of MSS experiments, in pseudo-second-order model, which gives more favourable results for the adsorption of AR dye in this study, are very close to  $q_{exp}^e$  values (Fig. 8).

Besides all that, while the AR dye concentration was decreased from 100 to 12.81 mg/L with 9.56 g/L of NSS, the final dye concentration decreased to 4.52 mg/L with 4.71 g/L of MSS at the end of the two hour experiment.

Consequently, MSS is an efficient and low-cost adsorbent to remove the astrazon red GTLN textile dye from the textile dying industry wastewaters.

#### Acknowledgement

This research was performed in the laboratories of Ataturk University, Engineering Faculty, Environmental Engineering Department.

#### References

- [1] P. Sine, Synthetic Dyes, first ed., Rajat Publications, New Delhi, 2003.
- [2] Y.S. Ho, G. McKay, Sorption of dyes and copper ions onto biosorbents, Process Biochem. 38 (2003) 1047–1061.

- [3] L.T. Markovska, V.D. Meshko, M.S. Marinkovski, Modeling of the adsorption kinetics of zinc onto granular activated carbon and natural zeolite, *J. Serb. Chem. Soc.* 71 (2006) 957–967.
- [4] M.T. Uddin, M.A. Islam, S. Mahmud, M. Rukanuzzaman, Adsorptive removal of methylene blue by tea waste, *J. Hazard. Mater.* 164 (2009) 53–60.
- [5] P. SenthilKumar, R. Gayathri, S. DineshKirupha, P. RajKumar, J. Nandagopal, S. Sivanesan, Adsorption of dye from aqueous solution using silver wood sawdust carbon, *Environ. Eng. Manage. J.* 10 (2011) 451–460.
- [6] S.R. Singh, A.P. Singh, Treatment of water containing chromium (VI) using rice husk carbon as a new low cost adsorbent, *Int. J. Environ. Res.* 6 (2012) 917–924.
- [7] F.B. AbdurRahman, M. Akter, M.Z. Abedin, Dyes removal from textile wastewater using orange peels, *Int. J. Sci. Technol. Res.* 2 (2013) 2277–8616.
- [8] D. Suteu, R. Lacramioara, Removal of methylene blue dye from aqueous solution using seashell wastes as biosorbent, *Environ. Eng. Manage. J.* 11 (2012) 1977–1985.
- [9] U.J. Etim, S.A. Umoren, U.M. Eduok, Coconut coir dust as a low cost adsorbent for the removal of cationic dye from aqueous solution, *J. Sau. Chem. Soc.* (in press) Corrected Proof, <http://dx.doi.org/10.1016/j.jscs.2012.09.014>.
- [10] K.A. Selim, M.A. Youssef, F.H. Abd El-Rahiem, M.S. Hassan, Dye removal using some surface modified silicate minerals, *Int. J. Min. Sci. Technol.* 24 (2014) 183–189.
- [11] M. Visa, A.M. Chelaru, Hydrothermally modified fly ash for heavy metals and dyes removal in advanced wastewater treatment, *Appl. Sur. Sci.* 303 (2014) 14–22.
- [12] Y. Peng, D. Chen, J. Ji, Y. Kong, H. Wan, C. Yao, Chitosan-modified palygorskite: Preparation, characterization and reactive dye removal, *Appl. Clay Sci.* 74 (2013) 81–86.
- [13] E. Alver, A.Ü. Metin, Anionic dye removal from aqueous solutions using modified zeolite: Adsorption kinetics and isotherm studies, *Chem. Eng. J.* 200–202 (2012) 59–67.
- [14] R.S.P. Couto, A.W.S. Guarino, Ch.W.C. Branco, E.F.A. Palermo, E.G. Azero, Application of clay minerals and polymeric resins to remove dissolved Microcystin-LR from water, *Int. J. Environ. Res.* 7 (2013) 435–442.
- [15] H. Tahir, M. Sultan, N. Akhtar, U. Hameed, T. Abid, Application of natural and modified sugar cane bagasse for the removal of dye from aqueous solution, *J. Sau. Chem. Soc.* (in press) corrected proof. <http://dx.doi.org/10.1016/j.jscs.2012.09.007>.
- [16] J.P. Lorimer, T.J. Mason, M. Plattes, S.S. Phull, D.J. Walton, Degradation of dye effluent, *Pure Appl. Chem.* 73 (2001) 1957–1968.
- [17] B. Kocadagistan, E. Kocadagistan, L. Gazioglu, Adsorption mechanism and removal capacity of sunflower seed shell for Astrazon Red GTLN basic dye, *Environ. Eng. Manage. J.* (in press) corrected proof.
- [18] H. Deng, J. Lu, G. Li, G. Zhang, X. Wang, Adsorption of methylene blue on adsorbent materials produced from cotton stalk, *Chem. Eng. J.* 172 (2011) 326–334.
- [19] P. Punjongharn, K. Meevasana, P. Pavasant, Influence of particle size and salinity on adsorption of basic dyes by agricultural waste: Dried seagrass (*Caulerpa lentillifera*), *J. Environ. Sci. (China)* 20 (2008) 760–768.
- [20] M.S. Abd-El-Kareem, H.M. Taha, Decolorization of malachite green and methylene blue by two microalgal species, *Int. J. Chem. Environ. Eng.* 3 (2012) 297–302.
- [21] R.P. Suresh Jeyakumar, V. Chandrasekaran, Adsorption of lead(II) ions by activated carbons prepared from marine green algae: Equilibrium and kinetics studies, *Int. J. Ind. Chem.* 5 (2014) 2–10.
- [22] G.O. El-Sayed, Removal of methylene blue and crystal violet from aqueous solutions by palm kernel fiber, *Desalination*. 272 (2011) 225–232.
- [23] H. Chen, J. Zhao, G. Dai, Silkworm exuviae—A new non-conventional and low-cost adsorbent for removal of methylene blue from aqueous solutions, *J. Hazard. Mater.* 186 (2011) 1320–1327.
- [24] S. Cengiz, F. Tanrikulu, S. Aksu, An alternative source of adsorbent for the removal of dyes from textile waters: *Posidonia oceanica* (L.), *Chem. Eng. J.* 189–190 (2012) 32–40.
- [25] A. Olad, F.F. Azhar, A study on the adsorption of chromium (VI) from aqueous solutions on the alginate-montmorillonite/polyaniline nanocomposite, *Desalin. Water Treat.* 52 (2014) 2548–2559.
- [26] M.E. Argun, S. Dursun, C. Ozdemir, M. Karatas, Heavy metal adsorption by modified oak sawdust: Thermodynamics and kinetics, *J. Hazard. Mater.* 141 (2007) 77–85.
- [27] X. Liu, D.-J. Lee, Thermodynamic parameters for adsorption equilibrium of heavy metals and dyes from wastewaters, *Bioresour. Technol.* 160 (2014) 24–31.
- [28] N. Thinakaran, P. Baskaralingam, M. Pulikesi, P. Panneerselvam, S. Sivanesan, Removal of Acid Violet 17 from aqueous solutions by adsorption onto activated carbon prepared from sunflower seed hull, *J. Hazard. Mater.* 151 (2008) 316–322.
- [29] Y. Guan, Y. Mao, D. Wei, X. Wang, P. Zhu, Adsorption thermodynamics and kinetics of disperse dye on poly(p-phenylene benzobisoxazole) fiber pretreated with polyphosphoric acid, *Korean J. Chem. Eng.* 30 (2013) 1810–1818.
- [30] S.C.R. Santos, R.A.R. Boaventura, Adsorption modeling of textile dyes by sepiolite, *Appl. Clay Sci.* 42 (2008) 137–145.
- [31] S. Chowdhury, R. Mishra, P. Saha, P. Kushwaha, Adsorption thermodynamics, kinetics and isosteric heat of adsorption of malachite green onto chemically modified rice husk, *Desalination* 265 (2011) 159–168.
- [32] P. Saha, S. Chowdhury, S. Gupta, I. Kumar, Insight into adsorption equilibrium, kinetics and thermodynamics of malachite green onto clayey soil of Indian origin, *Chem. Eng. J.* 165 (2010) 874–882.
- [33] V.K. Gupta, Suhas, Application of low-cost adsorbents for dye removal: A review, *J. Environ. Manage.* 90 (2009) 2313–2342.
- [34] R. Baccar, J. Bouzid, M. Feki, A. Montiel, Preparation of activated carbon from Tunisian olive-waste cakes and its application for adsorption of heavy metal ions, *J. Hazard. Mater.* 162 (2009) 1522–1529.